NIH Public Access
Author Manuscript
J Surg Res. Author manuscript; available in PMC 2015 August 01.

Published in final edited form as:
J Surg Res. 2014 August ; 190(2): 683–691. doi:10.1016/j.jss.2014.01.020.

Hind Limb Ischemia Reperfusion Injury in Diet Induced Obese Mice

Hassan Albadawi, MD[1,2], **Rahmi Oklu, MD. PhD**[1,3], **Nicholas R. Cormier**[2], **Ryan M. O'Keefe**[2], **James T. Heaton, PhD**[1,4], **James B. Kobler, PhD**[1,4], **William G. Austen, MD**[1,5], and **Michael T. Watkins, MD**

[1]Massachusetts General Hospital, Harvard Medical School, Boston, Massachusetts

[2]Department of Surgery, Division of Vascular and Endovascular Surgery, Boston, Massachusetts

[3]Department of Radiology, Division of Vascular Imaging and Intervention, Boston, Massachusetts

[4]Center for Laryngeal Surgery and Voice Rehabilitation, Boston, Massachusetts

[5]Division of Plastic and Reconstructive Surgery, Boston, Massachusetts

Abstract

Background—Obesity is a major risk factor for the development of diabetes. Limb ischemia reperfusion injury (IR) is a common clinical problem in diabetics who have compromised lower extremity perfusion. This study compared the histologic, metabolic and functional outcomes following hindlimb IR in diet-induced obese(DIO) and non-diabetic (ND) mice during the acute and the regenerative phases of IR.

Methods—DIO and ND mice were subjected to 1.5hrs unilateral hindlimb ischemia followed by 1 or 28 days IR. Muscle morphology, metabolic and genomic stress was evaluated at day 1 and 28 IR; Acute inflammation and thrombosis were only measured at day 1 IR. At day 28 IR, skeletal muscle contractility and maturation was also assessed.

Results—At day 1 IR, similar levels of acute muscle fiber necrosis were seen in both groups. DIO mice demonstrated substantially greater inflammatory, pro-thrombotic, and genomic stress responses which were also associated with a greater reduction in energy substrates and Akt

© 2014 Elsevier Inc. All rights reserved.

To Whom Correspondence is addressed: Hassan Albadawi, M.D., Massachusetts General Hospital, Division of Vascular and Endovascular Surgery, Vascular Research Laboratory, 70 Blossom Street, Boston, MA 02114, Phone: 617-724-7818, Fax: 617-726-2560, halbadawi@mgh.harvard.edu.

Publisher's Disclaimer: This is a PDF file of an unedited manuscript that has been accepted for publication. As a service to our customers we are providing this early version of the manuscript. The manuscript will undergo copyediting, typesetting, and review of the resulting proof before it is published in its final citable form. Please note that during the production process errors may be discovered which could affect the content, and all legal disclaimers that apply to the journal pertain.

Hassan Albadawi conception and design, data analysis, writing the article, critical revision
Rahmi Oklu: data analysis, writing the article
Nicholas R. Cormier data collection and data analysis
Ryan M. O'Keefe data collection and data analysis
James T. Heaton data analysis and writing the article
James B. Kobler data analysis and writing the article
William G. Austen: data analysis and writing the article
Michael T. Watkins conception and design, data analysis, writing the article

NIH-PA Author Manuscript
NIH-PA Author Manuscript
NIH-PA Author Manuscript

NIH-PA Author Manuscript

NIH-PA Author Manuscript

NIH-PA Author Manuscript

phosphorylation. At 28 days, there was no difference in the peak forces generated in the hindlimbs for the two groups. DIO mice had reduced fatigue resistance compared to ND and larger areas of fat accumulation even though there was no significant difference in muscle fiber maturation.

Conclusion—DIO mice had an exacerbated acute response to IR with enhanced metabolic deficit, fat accumulation and defective functional recovery during the regenerative phase of IR. These changes in fatigue resistance reflect compromised functional recovery following IR injury and have relevance for the functional recovery of patients with metabolic syndrome and insulin resistance.

Keywords

Limb ischemia; reperfusion injury; diabetes; diet-induced obesity; insulin resistance; muscle regeneration; inflammation; muscle contraction; metabolism; phosphoinositide-3-kinase–protein kinase B/Akt pathway

Introduction

Obesity and insulin resistance continue to increase worldwide and are considered to be the leading cause for developing Type II diabetes which is a risk factor for the development of peripheral arterial disease(1). Acute skeletal muscle ischemia-reperfusion injury (IR) frequently occurs in many clinical scenarios including lower extremity arterial disease, surgical interventions, circulatory shock and trauma. Advances in medical management through thrombolytic therapy or direct operative interventions improved limb salvage and functional recovery rates in most patients except for diabetics (1–4). Successful muscle regeneration following IR, is comprised of a degeneration phase, that include necrosis and inflammatory response aimed at removing damaged myofibers followed by a regenerative phase manifested by mobilization of the normally quiescent satellite cells. The satellite cells proliferate and migrate to the site of fiber injury, then fuse and differentiate to form new myofibers(5). However, compromised muscle regeneration in the context of diseased condition such as aging or diabetes may lead to impaired healing, permanent loss of muscle mass, and functional deficiency. Pathologically, normal muscle regeneration can be hampered by persistent and robust inflammation followed by fibrosis and significant lipid accumulation (6–8). Obesity or metabolic syndrome plays a significant in the development of type II diabetes and cardiovascular disease and the associated comorbidity (9–13).

Recently, experimental model of diet-induced obesity and insulin resistance has been developed to study type II diabetes as an alternative to the genetically-manipulated animal models. This is accomplished by feeding rodents diet containing 40–60% fat for at least 8 weeks. However, this model presents insulin resistance without pancreatic beta cell failure, which can be compensated by a marked beta cell proliferation (14, 15). This study was designed to evaluate the effect of the metabolic syndrome and insulin resistance on skeletal muscle acute and regenerative response following IR in DIO mice induced by prolonged high fat diet compared to ND mice.

NIH-PA Author Manuscript

NIH-PA Author Manuscript

NIH-PA Author Manuscript

Materials and Methods

Animal Protocol

Animal care and experimental procedures were in compliance with the "Principal of Laboratory Animal Care" (Guide for the Care and Use of Laboratory Animals, National Institutes of Health publication 86-23, 1985) and approved by the Institutional Review Committee. Age matched C57BL6 male mice acquired from Jackson Laboratory (Bar Harbor, ME) after being fed either 10%kcal fat diet (ND, n=13) or 60%kcal high fat diet (DIO, n=12) for 26 weeks. The DIO mice were characterized to be obese and have glucose intolerance, and moderate hyperinsulinemia, hyperglycemia and hyperlipidemia. A hind limb murine ischemia-reperfusion model (IR) was created as previously described (16). Briefly, following anesthesia, a calibrated rubber band was applied to the hind limb to induce 1.5 hours of ischemia and then removed to initiate reperfusion. At the end of 1 day or 28 days reperfusion, hindlimbs perfusion was documented with laser Doppler imaging and the ratio of the injured to the non-injured contralateral hindlimb perfusion was calculated. DIO (n=6) and ND (n=6) Sham mice from each group subjected to anesthesia alone were used as baseline controls. Mice were sacrificed and hindlimb tissues were collected and were fixed with Paraformaldehyde and imbedded in acrylic or paraffin for histologic analysis or immediately frozen in liquid nitrogen and stored at −80°C until analyzed. A separate group of DIO (n=12) and ND (n=12) mice were subjected to 1.5 hours ischemia and 28 days reperfusion or sham conditions followed by direct muscle electrical stimulation to study hindlimb function under sham condition or after 28 days reperfusion as described below.

Histology and morphometric analysis: to determine changes in muscle fiber morphology, 2μm thick acrylic imbedded cross sections taken at 1 day after IR from the middle portion of the tibialis anterior (TA) muscle. The muscle sections were stained with Mason's trichrome. Randomized 200× magnification digital images were recorded and examined by blinded observer as previously described(17). In the acute IR groups the injured and non-injured muscle fibers were sorted and expressed as a percent of the total number of fibers counted per field as previously described(18). In the 28 days groups, evidence of skeletal muscle fiber maturation in the TA muscle was evaluated by measuring the averages of muscle fiber cross sectional area (CSA), and adipocytes area in addition to counting the number of fibers presenting central nucleus as an indication of muscle fibers regeneration as has been described before (19). H&E or Oil Red O staining was performed on 2μm acrylic imbedded cross section or 8μm frozen section from each TA muscle. A minimum of ten randomized high power fields from each muscle cross section were evaluated by a blinded reviewer.

Local Markers of Inflammation

Selected markers of inflammation were measured in solubilized proteins obtained from hindlimb muscle after 1 day IR using quantitative sandwich enzyme immunoassays for the CXC chemokine, Keratinocyte Chemoattractant Protein (KC, (R&D Systems, Minneapolis, MN), and myeloperoxidase (mouse MPO; Cell Sciences, Canton, MA).

NIH-PA Author Manuscript

NIH-PA Author Manuscript

NIH-PA Author Manuscript

Assessment of Neutrophil Granulocytes Infiltration

5μm cross sections taken from the mid part of paraffin imbedded TA muscles were deparaffinized and rehydrated according to standard protocols. Sections were subjected to immunohistochemistry using monoclonal rat anti-mouse Ly6B.2 IgG (1:1000 dilutions, MCA771GA, AbD Serotec) over night at 4°C. The antibody recognizes the 40kDa alloantigen expressed by polymorphonuclear cells. Sections were then incubated with rabbit anti-rat biotinylated secondary antibody (1:300 dilutions, Vector laboratories) for 20 minutes followed by incubation with ABC complex (Vector Laboratories) for 30 minutes. The signal was visualized by reacting the 3,3'-Diaminobenzidine chromogenic substrate (DAB solution, Vector Laboratories). The average numbers of positive cells per slide were counted by a blinded reviewer in ten randomized fields obtained from each section at 200× magnification.

Muscle Adenosine Triphosphate (ATP) Quantification

ATP levels were measured using the ATPlite luminescence assay (PerkinElmer Life, Boston, MA) following the manufacturer's instructions as previously described (20). Protein concentrations were measured in the precipitates after acid neutralization and protein extraction. ATP levels were expressed as nanomoles per mg of total protein level.

Assessment of poly(ADP)-Ribosylated proteins and phosphorylated-Akt

50–100 μg total protein isolated from each hind-limb tissue using RIPA buffer supplemented with phosphates and protease inhibitors cocktail. The protein samples were mixed with an equal volume of Laemmli sample buffer, boiled for 5 min, loaded onto Tris-HCl-SDS gel and subjected to electrophoresis and electro-blotting transfer. PARP activity was assessed by western blotting, for the level of solubilized poly(ADP)-ribosylated proteins (PAR) using monoclonal anti-poly(ADP)-Ribose moiety antibody at 1:2000 (Tulip Biolabs, West Point, PA), as previously described(18). To assess Akt pathway activity, western blot membranes were probed with polyclonal antibodies specific for phosphorylated Serine-473 of the Akt proteins (pS473-Akt, 1:1000 dilutions, Cell Signaling). The specific band integrated density values were measured using the imaging system software which then normalized to the bands densities visualized after staining the membrane with Ponceau S.

Measurement of GAPDH Activity

GAPDH activity was evaluated on hindlimb muscle tissue extracts else were normalized to total protein and expressed as unit/2 mg protein as has been described(18).

Direct Muscle Electrical Stimulation

Hindlimb muscle contractile forces were determined as has been previously described (21). In brief, mice were anesthetized with 40–50mg/kg Pentobarbital and maintained at 37°C using radiant heat. The sciatic nerve was severed to prevent retrograde stimulation. The leg was immobilized with 4-0 silk suture binding the tibia to a stainless steel metal rod mounted on a platform. The third metatarsal was sutured to a TSD 105A force transducer (Biopac Systems) using 4-0 silk. Two Grass E2 platinum subdermal needle electrodes were placed through the Gastrocnemius muscle at a separation distance of 5 mm. Five-volts square waves pulses with duration of 5 ms were delivered at intervals of 500 ms through the

NIH-PA Author Manuscript

NIH-PA Author Manuscript

NIH-PA Author Manuscript

electrodes using STM100C (Biopac Systems). The animals were stimulated for 10 min. Tension from the force transducer was recorded with DA100C system and plotted using a UM100A and MP150 system with Acknowledge software (Biopac Systems). Peak force and fatigue force after 10 min of stimulation were measured. Sham animals subjected to anesthesia alone were used for baseline values to which the IR groups were compared.

Statistical analysis

Statistical analysis was performed with Instat (Graph pad, San Diego, CA) using parametric or non-parametric unpaired t-test or ANOVA. The results are expressed as the average ± standard error of the mean.

Results

Assessment of hind limb perfusion and acute muscle fiber injury following IR

Representative histology images of the reperfused skeletal muscle from ND and DIO groups are shown in Fig 1 images A and B, respectively. There was no difference in the hind limb perfusion ratios between ND and DIO groups at day 1 following IR (Table 1). Similarly, TA muscle of ND and DIO mice subjected to hindlimb IR revealed no significant difference in the percentage of injured muscle fibers between the two groups at day 1 (Table 1). These data suggest that diet-induced obesity neither alters tissue perfusion nor affects acute muscle fiber ischemic injury during the degenerative phase of IR.

Assessment of the inflammatory response during acute IR

Proinflammatory CXC chemoattractant, KC and MPO in the hindlimb muscle tissue protein extracts from ND and DIO mice were quantified. There were significantly higher levels of KC and MPO at day 1 after IR (KC: P=0.008 and MPO: P=0.0013, Table 1). These findings suggest that diet-induced obesity led to a state of greater inflammatory response compared to ND group. To further explore whether these differences correlated with the degree of leukocyte infiltration, the tissue sections were stained for the marker of Neutrophils, Ly6b and positive cells were counted (Fig 1. Images C and D). This analysis showed significantly higher infiltrating neutrophil granulocytes into the endomysium and perimysium of the DIO skeletal muscle compared to ND at day 1 following IR (P=0.00017, Table 1) indicating, increased neutrophil recruitment to the injured muscle. To determine whether this increased inflammatory responses will possibly be associated with increased markers of thrombosis, we quantified the level of thrombin-antithrombin III complex (TAT III) formation in the hind limb tissues following IR. This analysis revealed significantly higher TAT III levels in the DIO mice compared to ND (P=0.0005. Table 1) suggesting a higher prothrombotic milieu in the DIO tissue after acute injury.

Assessment of Metabolic and Genomic stress responses following IR

To evaluate the state of muscle fiber metabolic activity in response to IR injury between the two groups, the steady state levels of the energy substrate ATP was measured. ATP levels were measured in the hindlimb muscle at day 1 and 28 days following IR as well as in sham mice in both groups. The DIO sham mice muscle contained significantly less ATP substrate compared to ND group (ND Sham: 17.5±1.5, DIO Sham: 9.6±2.5 nmol/mg protein,

NIH-PA Author Manuscript

NIH-PA Author Manuscript

NIH-PA Author Manuscript

p=0.022) thus the results for the 1 and 28 Day IR were then normalized to their respective sham samples and expressed as percent sham. ATP levels fell to 30% of sham levels in the muscle from the ND group and to 36% in the DIO mice indicating lower available energy source in the obese mice (ATP 1 day; ND: 29.73±3.3 vs. DIO: 3.8±1.2 percent sham, P<0.01, Fig. 2). After 28 days IR the ATP levels in the ND mice recovered to baseline while the DIO mice showed significantly lower percent of ATP compared to ND (ND 28 Days IR: 119.3±9.9, DIO 28 Days IR: 75.7±6.7 sham. p<0.001, Fig. 2). As a further measure of metabolic stress, GAPDH activity was measured revealing similar levels under sham condition in the two groups (ND Sham: 0.93±0.03, DIO Sham: 1.0±0.04 U/2mg total protein. p=0.238, Fig. 3). However GAPDH activity dropped significantly lower after 1 day IR in the DIO mice compared to ND (ND: 0.18±0.028 vs. DIO: 0.069±0.008 Unit/2mg protein. p<0.01, Fig. 3). In contrast by 28 days following IR, GAPDH activity recovered close to sham levels in both groups but was significantly higher in the DIO group (ND: 0.79±0.016 vs. DIO: 0.98±0.02 U/2mg total protein. p<0.001, Fig. 3).

Since PARP activation has been associated with cellular stress and metabolic substrate depletion in response to several pathologic conditions including IR (20, 22), PARP activity at day 1 and day 28 following IR were measured. Analysis of tissue protein extracts revealed higher levels of poly(ADP)-Ribosylated proteins in the DIO group compared to the ND group at day 1 (ND: 3.05±0.5 vs. DIO: 4.97±0.39, AU, P<0.01) and at day 28 (ND: 2.08±0.13, DIO: 3.17±0.42 AU, p<0.01) following IR, indicating higher PARP activity (Fig. 4).

Assessment of Akt pathway activity following IR

There was no difference in Akt phosphorylation (pS473-Akt) under sham condition between the two groups (ND: 11.18±1.8 vs. DIO: 11.15±1.19. p=0.99). However, significantly lower Akt phosphorylation was detected in the DIO group at day 1 (1 Day IR, ND: 7.8±1.7 vs. DIO: 4.2±0.2 AU. P<0.01) and day 28 (28 Days IR, ND: 6.8±0.60 vs. DIO: 4.5±0.3 AU p<0.01) following IR (Fig. 5A and 5B).

Skeletal muscle fiber regeneration following IR

Histologic evaluation of skeletal muscle tissue during the regenerative phase of reperfusion injury (28 days following IR) revealed greater fat accumulation in the DIO mice (P=0.005, Fig. 6 and Table 2) and significantly lower percent of fibers presented with centrally located nuclei (P=0.0026, Table 2). Furthermore, a comparison of the average skeletal muscle fiber cross sectional area in the DIO mice compared to ND revealed marginally higher average cross sectional area in the DIO mice but the data did not reach statistical significance (P=0.69, Table 2). These results suggest that the regenerative phase of IR in DIO mice diverges to favor greater non-contractile fat accumulation in the injured tissues.

Skeletal muscle contractility during the regenerative phase of IR

There was no difference in the measured peak and fatigue forces between the DIO and ND sham mice (Sham peak Force: ND; 160.8±4.6 vs. DIO; 148.0±10.8 grams, p=0.25) (Sham fatigue Force: ND; 53.1±7.4 vs. DIO; 50.4±1.8 grams. P=0.78) as assessed by hind limb direct muscle stimulation. The peak forces generated after IR were significantly lower than

NIH-PA Author Manuscript

NIH-PA Author Manuscript

NIH-PA Author Manuscript

the respective sham mice in both groups by ~50% lower indicating that the mice still did not fully recover its potential contractile force strength after 28 days IR. Measurements of the average peak forces in ND and DIO mice at 28 days following IR were not different (ND: 84.152±2.5, DIO: 84.35±3.46 grams. p=0.96, Fig. 7). However, the fatigued forces toward the end of the 10 minutes stimulation period were significantly lower in the DIO mice compared to ND group (ND: 47.4±5.68, DIO: 24.24±6.19 grams. p=0.022, Fig. 7).

Discussion

Skeletal muscle regeneration and functional recovery are important components of the limb salvage following revascularization procedures in type 2 diabetic patients. Since studying the early stages of diabetes and the ensuing morbidities is difficult in humans, investigators have utilized animal models of diet-induced obesity to replicate the condition of insulin resistance and metabolic syndrome observed in human type II diabetics(23). In this study we investigated the effect of diet-induced obesity on the acute and regenerative phase of hind limb ischemia reperfusion injury in mice that were fed high fat diet (24). Our findings indicate a substantially greater degree of inflammation and metabolic derangement along with evidence of exacerbated genomic stress associated with diet-induced obesity. Despite this, we found a similar degree of skeletal muscle fiber injury in the hind limb muscle of both groups during the acute phase of reperfusion. There was a more profound reduction in tissue ATP levels in addition to reduced GAPDH and Akt pathway activities after 1 day IR as compared to ND mice. The decrease in GAPDH activity was association with an increase in PARP activity and enhanced ATP depletion in skeletal muscle of DIO mice. We hypothesize that the DIO mice had increased oxidative stress during acute reperfusion. This stress could incite the activation of the nuclear enzymes, poly(ADP)-Ribose polymerases (PARPs) which leads to depletion of NAD+, thereby slowing the rate of glycolysis and the activity of the electron transport system, and thus ATP formation. In addition, we have reported that PARP activity can poly(ADP)ribosylate GAPDH as a form of post-translational modification and inhibit its activity after acute hind limb IR in Db/Db mice(18), which was also confirmed in different tissues and reviewed by other investigators (25–27). In the second part of this study we focused on the regenerative phase of IR injury, by comparing histologic indices of skeletal muscle fiber maturation and markers of functional recovery following hind limb ischemia in DIO and ND mice. Skeletal muscle fibers are multinucleated cells within a continuous cytoplasm that are able to replicate following a variety of different injuries through a complicated process that involves the fusion and differentiation of mononucleated precursor cells, derived primarily from satellite cells. Several studies of skeletal muscle regeneration have used different models of injury, including myotoxic agents. However, recent literature demonstrated that acute IR injury in mice induces more detrimental effects on skeletal muscle than cardiotoxin injury and causes long-term delayed recovery (28, 29). Our results revealed marginal differences in the histologic indices of muscle fiber maturation during the regenerative phase of IR with a slight increase in muscle fiber cross-sectional area and fewer fibers presenting with centrally located nuclei in the DIO mice compared to ND mice. One possible explanation for the lack of histologic differences is that the degree of metabolic syndrome in these mice may not have been severe enough to cause marked structural changes and impair regenerative

NIH-PA Author Manuscript

NIH-PA Author Manuscript

NIH-PA Author Manuscript

capacity after IR injury. This finding is in agreement with what has been reported in leptin-deficient mice (Db/Db and Ob/Ob strains) subjected to cardiotoxin muscle injury. These mice had impaired muscle regeneration compared to high-fat-diet mice (29). It may be necessary to feed the mice a diet that contains high glucose in addition to high fat. It has been shown that mice on a diet high in fat and fructose had impaired angiogenic response in the hind limb following ligation of the femoral artery (30). Another possible explanation for the similarity in the degree of muscle fiber injury and muscle regeneration is that the degree of ischemic insult could have been too mild. A longer duration of ischemia (i.e. >1.5 hours) might be needed to reveal significant histologic effects in this model. Additional findings in this study revealed that regenerating muscle of DIO mice contained larger areas of fat accumulation compared to ND group with persistently marked decrease in the steady sate level of muscle ATP and Akt activity with increased PARP activity compared 28 days following IR. The link between the intra-muscular lipid accumulation and impaired glucose intolerance and insulin resistance and the resulting oxidative stress and metabolic derangement has been established for diabetic patients (31–35). The mechanism by which lipid accumulation in the muscle induces insulin resistance is still under investigation. Studies used cultured myotubes from humans suggest that reduced muscle fiber oxidative capacity results in failure to oxidize lipid intermediates to generate free fatty acids (36, 37). The serine-threonine protein kinase Akt pathway or protein kinase B is an important downstream mediator of the insulin receptor pathway for the maintenance of glucose homeostasis, and plays a central role in maintaining insulin sensitivity in humans (38). Detecting changes in Akt phosphorylation in the pS473 and pT308 sites has been used to gauge Akt pathway signaling and changes in insulin sensitivity (39, 40). Our results showed no difference in the baseline levels of Akt phosphorylation between the two groups. However, Akt pathway signaling is reduced during the acute phase of IR and starts to recover to the sham levels during the regenerative phase of IR. pS473-Akt was relatively low during both the acute and regenerative phase in the DIO mice compared to the ND mice. These data are in agreement with a previous report that muscle damage enhances local insulin resistance by compromising IRS-1 and PI3-Akt pathway activity in humans (41). Other investigators reported that high fat diet impaired PI3K/Akt signaling in rat liver (42). These findings prompted us to undertake an analysis of hind limb contractile function using direct muscle stimulation. Results revealed that the DIO condition had no influence on the contractile capacity of the hind limb in non-injured sham mice. These results are in agreement with observations that DIO have impaired oxidative capacity that is insufficient to impact muscle contractility compared to ND mice(43). However, following IR the DIO mice had similar peak forces but experienced reduced fatigue resistance at the end of the stimulation period. These findings that DIO mice have similar contractile machinery but due to the metabolic dysfunction and insulin resistance they were not able to maintain adequate force in the long-term compared to ND mice. It has been established that aged diabetic patients experience decreased muscle function and quality of life (44, 45). This data is consistent with our histologic and molecular findings in the DIO, where we found concomitant decrease in muscle ATP, reduced PI3-Akt activity, increased PARP activity and lipid accumulation.

NIH-PA Author Manuscript

NIH-PA Author Manuscript

NIH-PA Author Manuscript

Conclusion

Our findings suggest that diet-induced obesity affects the degenerative phase following IR, setting a course for exacerbated intramuscular fat accumulation and local insulin resistance. In the long term, these effects cause further local metabolic derangement and decreased fatigue resistance in the affected muscles. Detailed studies aimed at investigating the mechanisms responsible for enhanced muscle insulin resistance, altered muscle regeneration and functional recovery in diet induced obesity following IR is warranted. This will help to identify molecular targets for therapeutic interventions to enhance functional recover in diabetic patients recovering from acute or chronic limb ischemia/reperfusion.

Acknowledgments

MTW is the Isenberg Scholar in Academic Surgery at the Massachusetts General Hospital. This study was supported by NIH grant RO1 AR055843 (MTW), Pacific Vascular Research Foundation, the Department of Surgery, Division of Vascular and Endovascular Surgery (The Rosenberg Fund). RO is funded by the American College of Phlebology and the Department of Radiology, Division of Vascular Imaging and Intervention.

References

1. Abularrage CJ, Conrad MF, Hackney LA, Paruchuri V, Crawford RS, Kwolek CJ, LaMuraglia GM, Cambria RP. Long-term outcomes of diabetic patients undergoing endovascular infrainguinal interventions. J Vasc Surg. 2010; 52:314–322. e311–e314. [PubMed: 20591601]
2. Engelhardt M, Bruijnen H, Scharmer C, Jezdinsky N, Wolfle K. Improvement of quality of life six months after infrageniculate bypass surgery: diabetic patients benefit less than non-diabetic patients. Eur J Vasc Endovasc Surg. 2006; 32:182–187. [PubMed: 16567116]
3. Engelhardt M, Bruijnen H, Scharmer C, Wohlgemuth WA, Willy C, Wolfle KD. Prospective 2-years follow-up quality of life study after infrageniculate bypass surgery for limb salvage: lasting improvements only in non-diabetic patients. Eur J Vasc Endovasc Surg. 2008; 36:63–70. [PubMed: 18356087]
4. Nguyen LL, Moneta GL, Conte MS, Bandyk DF, Clowes AW, Seely BL. Prospective multicenter study of quality of life before and after lower extremity vein bypass in 1404 patients with critical limb ischemia. J Vasc Surg. 2006; 44:977–983. discussion 983-974. [PubMed: 17098529]
5. Ciciliot S, Schiaffino S. Regeneration of mammalian skeletal muscle. Basic mechanisms and clinical implications. Curr Pharm Des. 2010; 16:906–914. [PubMed: 20041823]
6. Jelinek JS, Murphey MD, Aboulafia AJ, Dussault RG, Kaplan PA, Snearly WN. Muscle infarction in patients with diabetes mellitus: MR imaging findings. Radiology. 1999; 211:241–247. [PubMed: 10189479]
7. Cardillo S, Huse JT, Iqbal N. Diabetic muscle infarction of the forearm in a patient with long-standing type 1 diabetes. Endocr Pract. 2006; 12:188–192. [PubMed: 16690469]
8. Entabi F, Albadawi H, Stone DH, Sroufe R, Conrad MF, Watkins MT. Hindlimb ischemia-reperfusion in the leptin receptor deficient (db/db) mouse. J Surg Res. 2007; 139:97–105. [PubMed: 17292407]
9. Meigs JB. Epidemiology of type 2 diabetes and cardiovascular disease: translation from population to prevention: the Kelly West award lecture 2009. Diabetes Care. 2010; 33:1865–1871. [PubMed: 20668155]
10. Hu G, Qiao Q, Tuomilehto J, Balkau B, Borch-Johnsen K, Pyorala K. Prevalence of the metabolic syndrome and its relation to all-cause and cardiovascular mortality in nondiabetic European men and women. Arch Intern Med. 2004; 164:1066–1076. [PubMed: 15159263]
11. Conen D, Rexrode KM, Creager MA, Ridker PM, Pradhan AD. Metabolic syndrome, inflammation, and risk of symptomatic peripheral artery disease in women: a prospective study. Circulation. 2009; 120:1041–1047. [PubMed: 19738135]

NIH-PA Author Manuscript

NIH-PA Author Manuscript

NIH-PA Author Manuscript

12. Vlek AL, van der Graaf Y, Sluman MA, Moll FL, Visseren FL. Metabolic syndrome and vascular risk in patients with peripheral arterial occlusive disease. J Vasc Surg. 2009; 50:61–69. [PubMed: 19223144]
13. van Kuijk JP, Flu WJ, Chonchol M, Bax JJ, Verhagen HJ, Poldermans D. Metabolic syndrome is an independent predictor of cardiovascular events in high-risk patients with occlusive and aneurysmatic peripheral arterial disease. Atherosclerosis. 2010; 210:596–601. [PubMed: 20056224]
14. Surwit RS, Kuhn CM, Cochrane C, McCubbin JA, Feinglos MN. Diet-induced type II diabetes in C57BL/6J mice. Diabetes. 1988; 37:1163–1167. [PubMed: 3044882]
15. Winzell MS, Ahren B. The high-fat diet-fed mouse: a model for studying mechanisms and treatment of impaired glucose tolerance and type 2 diabetes. Diabetes. 2004; 53(Suppl 3):S215–S219. [PubMed: 15561913]
16. Crawford RS, Hashmi FF, Jones JE, Albadawi H, McCormack M, Eberlin K, Entabi F, Atkins MD, Conrad MF, Austen WG Jr, Watkins MT. A novel model of acute murine hindlimb ischemia. Am J Physiol Heart Circ Physiol. 2007; 292:H830–H837. [PubMed: 17012358]
17. McCormack MC, Kwon E, Eberlin KR, Randolph M, Friend DS, Thomas AC, Watkins MT, Austen WG Jr. Development of reproducible histologic injury severity scores: skeletal muscle reperfusion injury. Surgery. 2008; 143:126–133. [PubMed: 18154940]
18. Long CA, Boloum V, Albadawi H, Tsai S, Yoo HJ, Oklu R, Goldman MH, Watkins MT. Poly-ADP-Ribose-Polymerase Inhibition Ameliorates Hindlimb Ischemia Reperfusion Injury in a Murine Model of Type 2 Diabetes. Ann Surg. 2013
19. Contreras-Shannon V, Ochoa O, Reyes-Reyna SM, Sun D, Michalek JE, Kuziel WA, McManus LM, Shireman PK. Fat accumulation with altered inflammation and regeneration in skeletal muscle of CCR2−/− mice following ischemic injury. Am J Physiol Cell Physiol. 2007; 292:C953–C967. [PubMed: 17020936]
20. Crawford RS, Albadawi H, Atkins MD, Jones JE, Yoo HJ, Conrad MF, Austen WG Jr, Watkins MT. Postischemic poly (ADP-ribose) polymerase (PARP) inhibition reduces ischemia reperfusion injury in a hind-limb ischemia model. Surgery. 2010; 148:110–118. [PubMed: 20132957]
21. Paoni NF, Peale F, Wang F, Errett-Baroncini C, Steinmetz H, Toy K, Bai W, Williams PM, Bunting S, Gerritsen ME, Powell-Braxton L. Time course of skeletal muscle repair and gene expression following acute hindlimb ischemia in mice. Physiol Genomics. 2002; 11:263–272. [PubMed: 12399448]
22. Szabo G, Bahrle S. Role of nitrosative stress and poly(ADP-ribose) polymerase activation in myocardial reperfusion injury. Curr Vasc Pharmacol. 2005; 3:215–220. [PubMed: 16026318]
23. Islam MS, Wilson RD. Experimentally induced rodent models of type 2 diabetes. Methods Mol Biol. 2012; 933:161–174. [PubMed: 22893406]
24. Galgani JE, Uauy RD, Aguirre CA, Diaz EO. Effect of the dietary fat quality on insulin sensitivity. Br J Nutr. 2008; 100:471–479. [PubMed: 18394213]
25. Devalaraja-Narashimha K, Padanilam BJ. PARP-1 inhibits glycolysis in ischemic kidneys. J Am Soc Nephrol. 2009; 20:95–103. [PubMed: 19056868]
26. Kiss L, Szabo C. The pathogenesis of diabetic complications: the role of DNA injury and poly(ADP-ribose) polymerase activation in peroxynitrite-mediated cytotoxicity. Mem Inst Oswaldo Cruz. 2005; 100(Suppl 1):29–37. [PubMed: 15962096]
27. Pacher P, Szabo C. Role of poly(ADP-ribose) polymerase-1 activation in the pathogenesis of diabetic complications: endothelial dysfunction, as a common underlying theme. Antioxid Redox Signal. 2005; 7:1568–1580. [PubMed: 16356120]
28. Vignaud A, Hourde C, Medja F, Agbulut O, Butler-Browne G, Ferry A. Impaired skeletal muscle repair after ischemia-reperfusion injury in mice. J Biomed Biotechnol. 2010; 2010:724–914.
29. Nguyen MH, Cheng M, Koh TJ. Impaired muscle regeneration in ob/ob and db/db mice. Scientific World Journal. 2011; 11:1525–1535. [PubMed: 21805021]
30. Kito T, Shibata R, Kondo M, Yamamoto T, Suzuki H, Ishii M, Murohara T. Nifedipine ameliorates ischemia-induced revascularization in diet-induced obese mice. Am J Hypertens. 2012; 25:401–406. [PubMed: 22223040]

NIH-PA Author Manuscript

NIH-PA Author Manuscript

NIH-PA Author Manuscript

31. van Hees AM, Jans A, Hul GB, Roche HM, Saris WH, Blaak EE. Skeletal muscle fatty acid handling in insulin resistant men. Obesity (Silver Spring). 2011; 19:1350–1359. [PubMed: 21331063]
32. Moors CC, van der Zijl NJ, Diamant M, Blaak EE, Goossens GH. Impaired insulin sensitivity is accompanied by disturbances in skeletal muscle fatty acid handling in subjects with impaired glucose metabolism. Int J Obes (Lond). 2011; 36:709–717. [PubMed: 21712806]
33. Clark BA, Alloosh M, Wenzel JW, Sturek M, Kostrominova TY. Effect of diet-induced obesity and metabolic syndrome on skeletal muscles of Ossabaw miniature swine. Am J Physiol Endocrinol Metab. 2011; 300:E848–E857. [PubMed: 21304063]
34. Corcoran MP, Lamon-Fava S, Fielding RA. Skeletal muscle lipid deposition and insulin resistance: effect of dietary fatty acids and exercise. Am J Clin Nutr. 2007; 85:662–677. [PubMed: 17344486]
35. Itani SI, Ruderman NB, Schmieder F, Boden G. Lipid-induced insulin resistance in human muscle is associated with changes in diacylglycerol, protein kinase C, and IkappaB-alpha. Diabetes. 2002; 51:2005–2011. [PubMed: 12086926]
36. Corpeleijn E, Hessvik NP, Bakke SS, Levin K, Blaak EE, Thoresen GH, Gaster M, Rustan AC. Oxidation of intramyocellular lipids is dependent on mitochondrial function and the availability of extracellular fatty acids. Am J Physiol Endocrinol Metab. 2010; 299:E14–E22. [PubMed: 20442319]
37. Moro C, Bajpeyi S, Smith SR. Determinants of intramyocellular triglyceride turnover: implications for insulin sensitivity. Am J Physiol Endocrinol Metab. 2008; 294:E203–E213. [PubMed: 18003718]
38. George S, Rochford JJ, Wolfrum C, Gray SL, Schinner S, Wilson JC, Soos MA, Murgatroyd PR, Williams RM, Acerini CL, Dunger DB, Barford D, Umpleby AM, Wareham NJ, Davies HA, Schafer AJ, Stoffel M, O'Rahilly S, Barroso I. A family with severe insulin resistance and diabetes due to a mutation in AKT2. Science. 2004; 304:1325–1328. [PubMed: 15166380]
39. Cho H, Mu J, Kim JK, Thorvaldsen JL, Chu Q, Crenshaw EB 3rd, Kaestner KH, Bartolomei MS, Shulman GI, Birnbaum MJ. Insulin resistance and a diabetes mellitus-like syndrome in mice lacking the protein kinase Akt2 (PKB beta). Science. 2001; 292:1728–1731. [PubMed: 11387480]
40. Jiang G, Dallas-Yang Q, Li Z, Szalkowski D, Liu F, Shen X, Wu M, Zhou G, Doebber T, Berger J, Moller DE, Zhang BB. Potentiation of insulin signaling in tissues of Zucker obese rats after acute and long-term treatment with PPARgamma agonists. Diabetes. 2002; 51:2412–2419. [PubMed: 12145152]
41. Del Aguila LF, Krishnan RK, Ulbrecht JS, Farrell PA, Correll PH, Lang CH, Zierath JR, Kirwan JP. Muscle damage impairs insulin stimulation of IRS-1, PI 3-kinase, and Akt-kinase in human skeletal muscle. Am J Physiol Endocrinol Metab. 2000; 279:E206–E212. [PubMed: 10893341]
42. Han JW, Zhan XR, Li XY, Xia B, Wang YY, Zhang J, Li BX. Impaired PI3K/Akt signal pathway and hepatocellular injury in high-fat fed rats. World J Gastroenterol. 16:6111–6118. [PubMed: 21182226]
43. Shortreed KE, Krause MP, Huang JH, Dhanani D, Moradi J, Ceddia RB, Hawke TJ. Muscle-specific adaptations, impaired oxidative capacity and maintenance of contractile function characterize diet-induced obese mouse skeletal muscle. PLoS One. 2009; 4:e7293. [PubMed: 19806198]
44. Park SW, Goodpaster BH, Strotmeyer ES, de Rekeneire N, Harris TB, Schwartz AV, Tylavsky FA, Newman AB. Decreased muscle strength and quality in older adults with type 2 diabetes: the health, aging, and body composition study. Diabetes. 2006; 55:1813–1818. [PubMed: 16731847]
45. Park SW, Goodpaster BH, Strotmeyer ES, Kuller LH, Broudeau R, Kammerer C, de Rekeneire N, Harris TB, Schwartz AV, Tylavsky FA, Cho YW, Newman AB. Accelerated loss of skeletal muscle strength in older adults with type 2 diabetes: the health, aging, and body composition study. Diabetes Care. 2007; 30:1507–1512. [PubMed: 17363749]

NIH-PA Author Manuscript
NIH-PA Author Manuscript
NIH-PA Author Manuscript

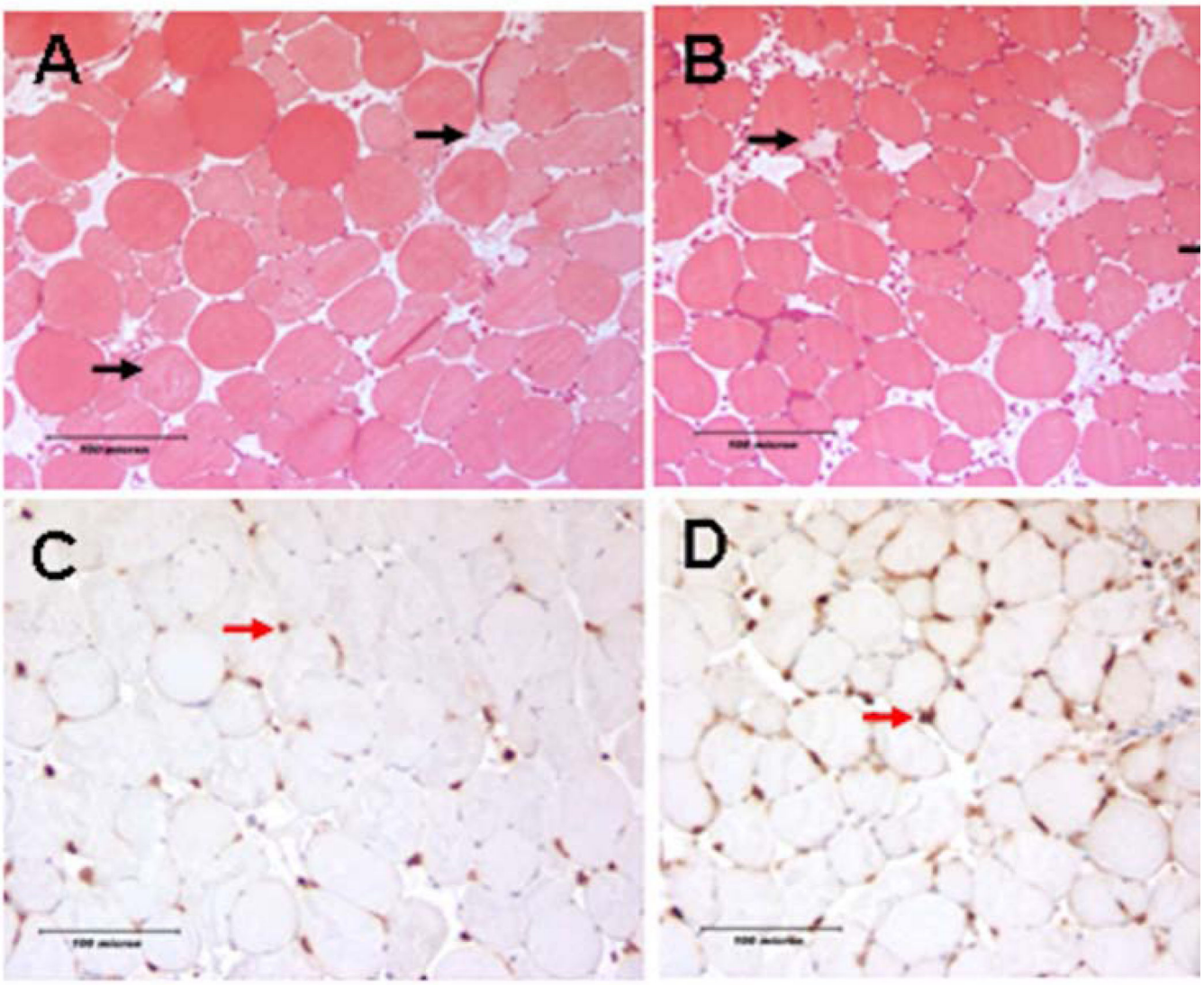

Figure 1. Histologic assessment of hind limb acute muscle fiber injury and neutrophil infiltration following acute IR

Images A and B are mason trichrome stained TA muscle cross sections taken from DIO or ND mice respectively obtained 24 hours following IR. Black arrows indicate injured skeletal muscle fibers in each field. Images C and D are Ly6B positive neutrophils (red arrow) in the TA muscle, taken from DIO and ND mice respectively. There was no difference in the average number acute of injured fiber between the two groups; however we identified markedly more infiltrating neutrophil granulocytes in the DIO muscles 24 hours after IR.

NIH-PA Author Manuscript

NIH-PA Author Manuscript

NIH-PA Author Manuscript

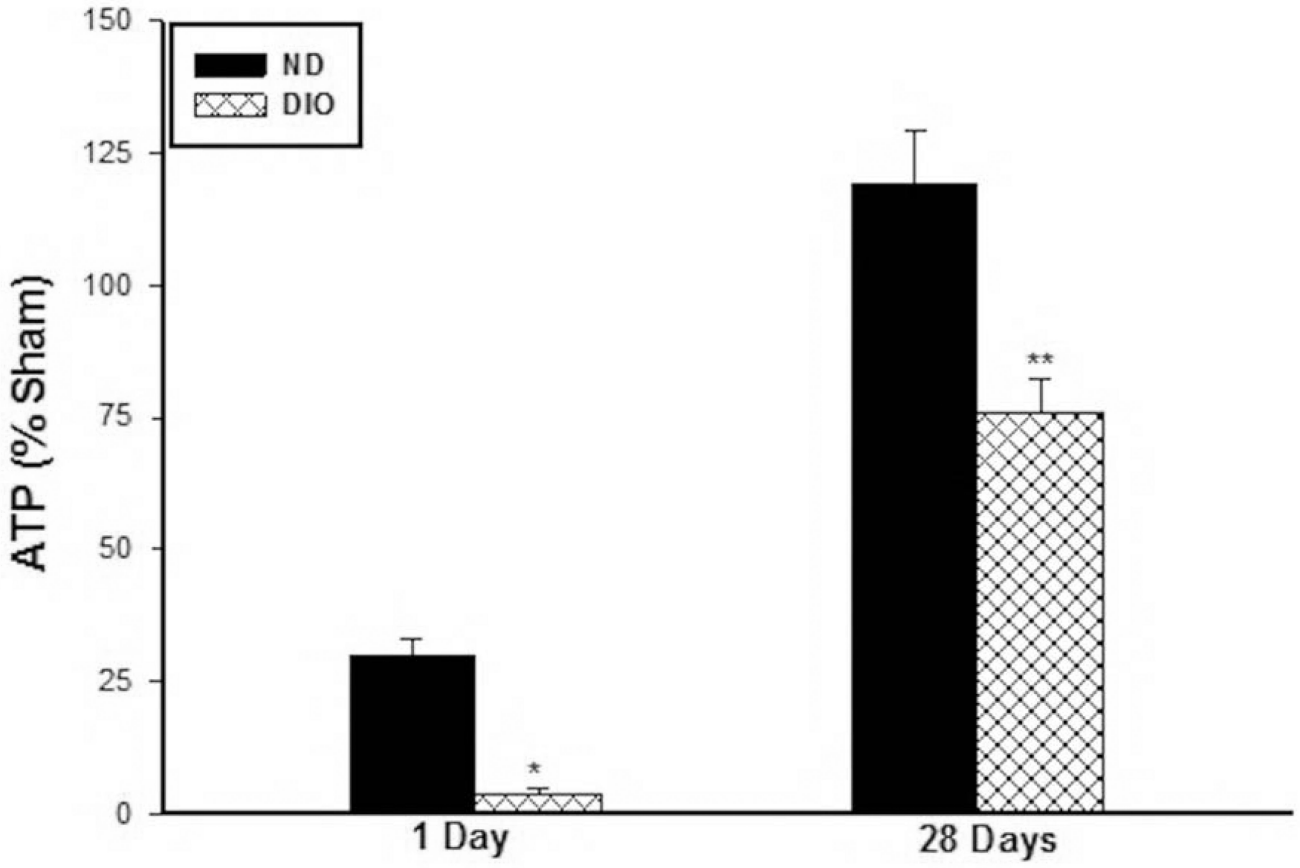

Figure 2. Skeletal muscle ATP levels

There significantly lower ATP percent in DIO mice after 1 day (* p P<0.01, n=6–7) and 28 days (**p<0.001, n=6) following IR compared to ND. ATP levels recovered to baseline sham levels in the ND group after 28 days IR while remained at 75 percent of sham levels in the DIO mice.

NIH-PA Author Manuscript
NIH-PA Author Manuscript
NIH-PA Author Manuscript

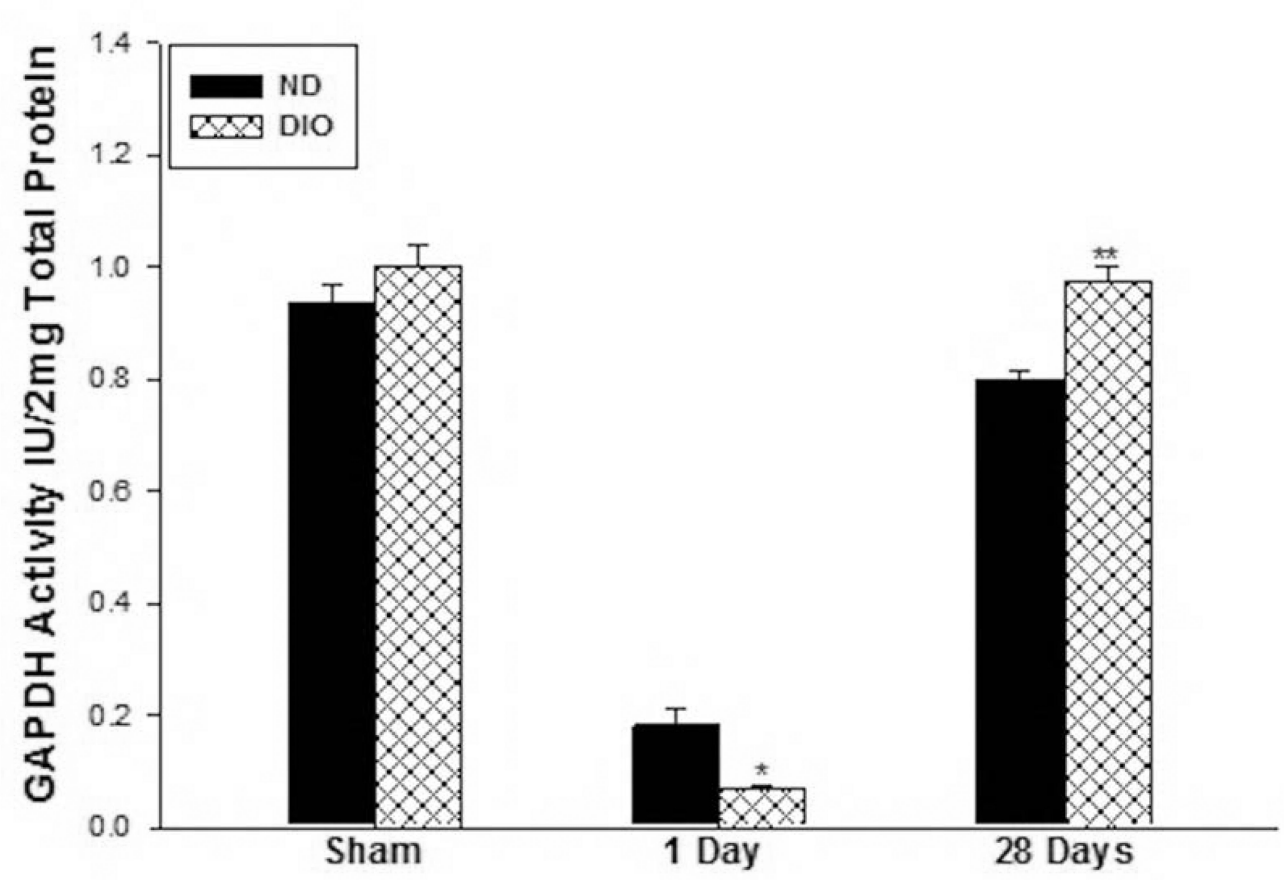

Figure 3. Skeletal muscle GAPDH activity following IR

There was no difference in GAPDH activity in the sham groups however after 1 day IR (n=6), GAPDH activity was significantly lower in the DIO mice (*$p<0.01$, n=6–7). In contrast, by 28 days IR GAPDH activity was significantly higher in the DIO group (** $p<0.001$, n=6).

NIH-PA Author Manuscript

NIH-PA Author Manuscript

NIH-PA Author Manuscript

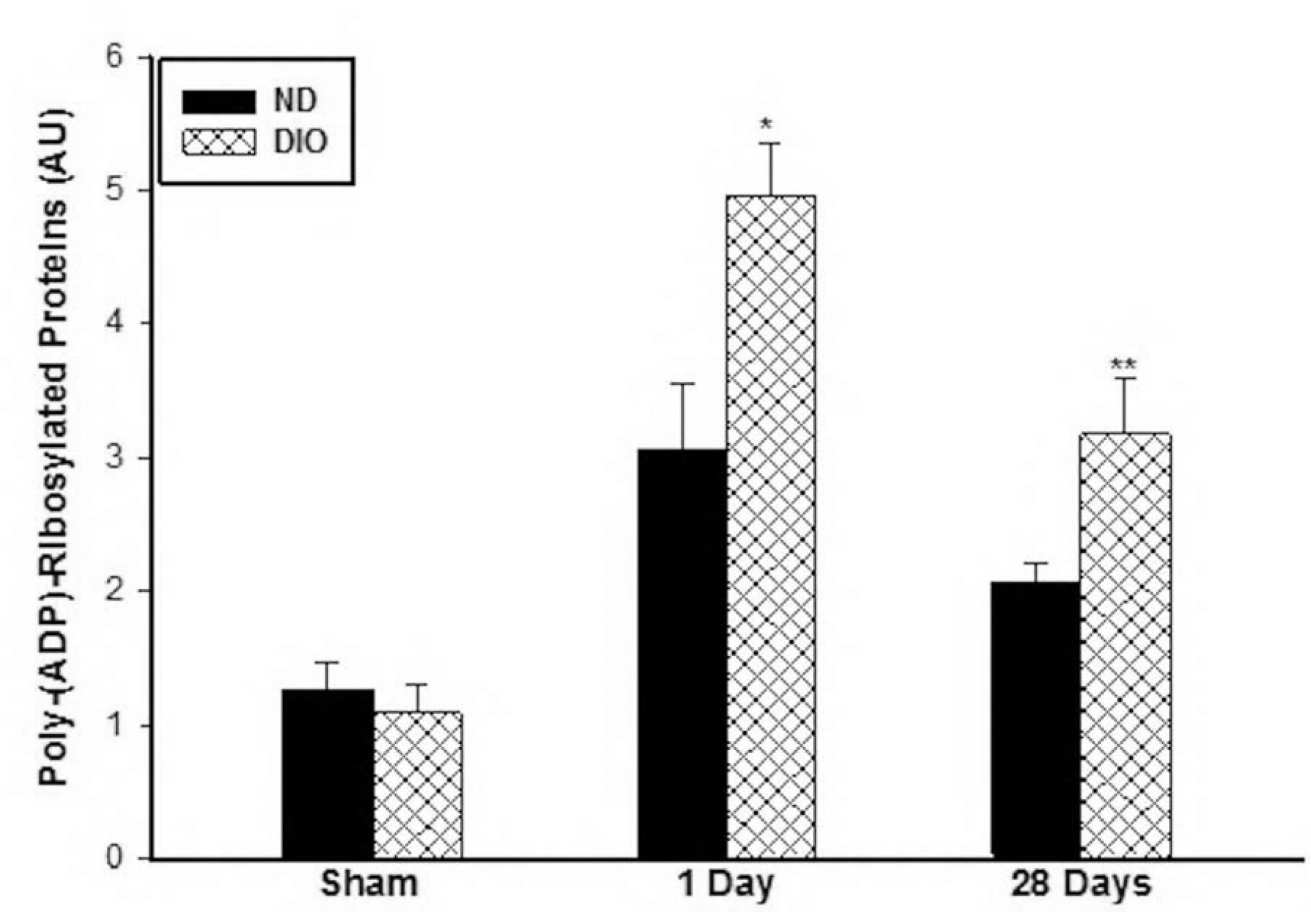

Figure 4. Skeletal muscle PARP activity under sham conditions and following IR

PARP activity was evaluated by comparing the levels of poly(ADP)-Ribosylated proteins. There was no significant difference in the levels of poly(ADP)-Ribosylated proteins under in sham muscle protein extract. However, the levels of poly ADP ribosylated proteins was significantly higher at 1 (n=6–7) and 28 days (n=6) following IR (*,** $p<0.01$).

NIH-PA Author Manuscript

NIH-PA Author Manuscript

NIH-PA Author Manuscript

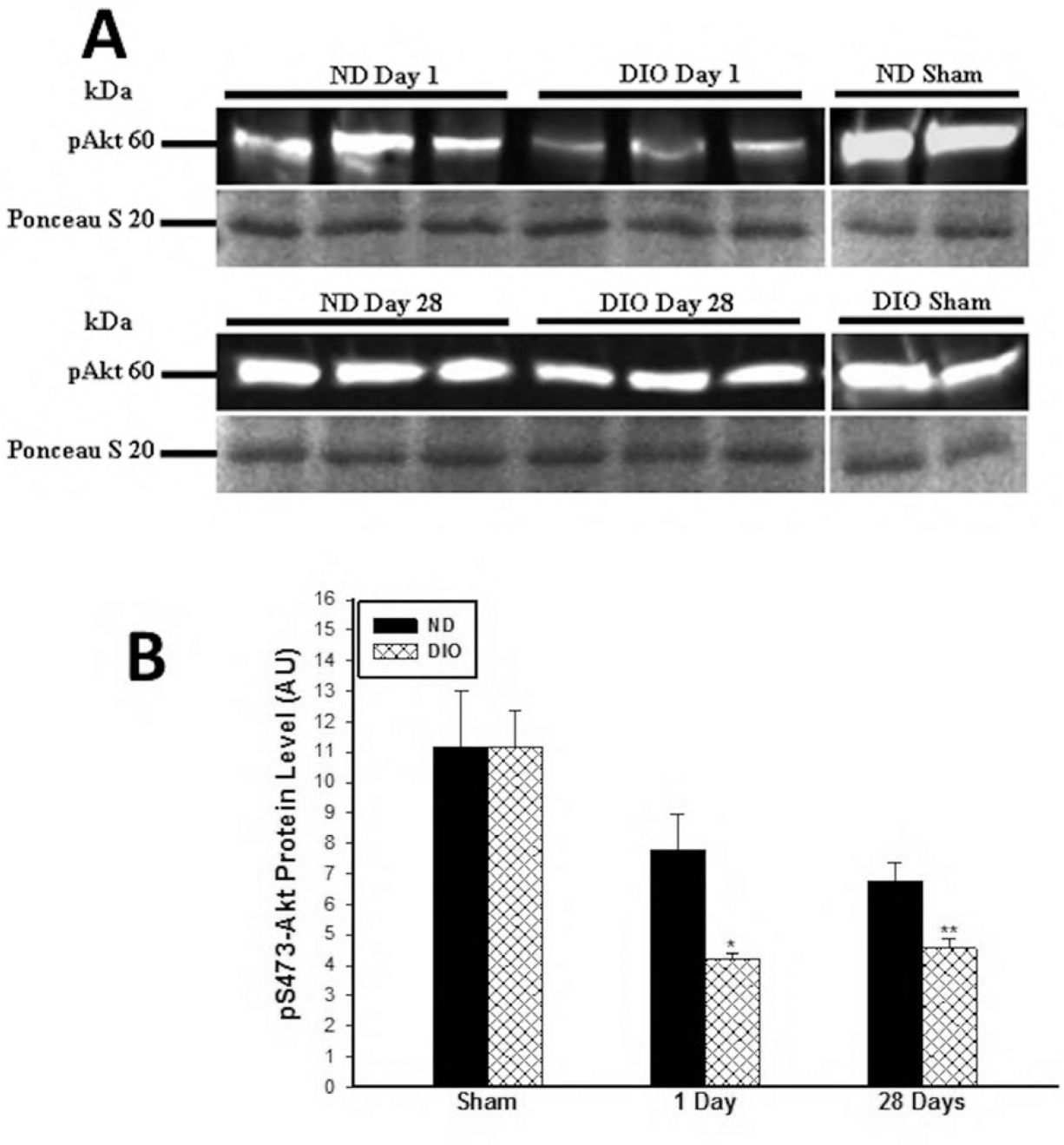

Figure 5. A. Representative western blot image for phosphorylated-S473-Akt in soluble skeletal muscle protein samples obtained at 1 and 28 days following IR. B. Assessment of Akt pathway activity at 1 and 28 days following IR

There was no difference in phosphorylated Serine 473-Akt under sham condition. However by 1 and 28 days after IR there was significantly lower pS473 expression in the DIO mice or 28 days following IR compared to ND (*,** $p<0.01$, n=6–7).

NIH-PA Author Manuscript
NIH-PA Author Manuscript
NIH-PA Author Manuscript

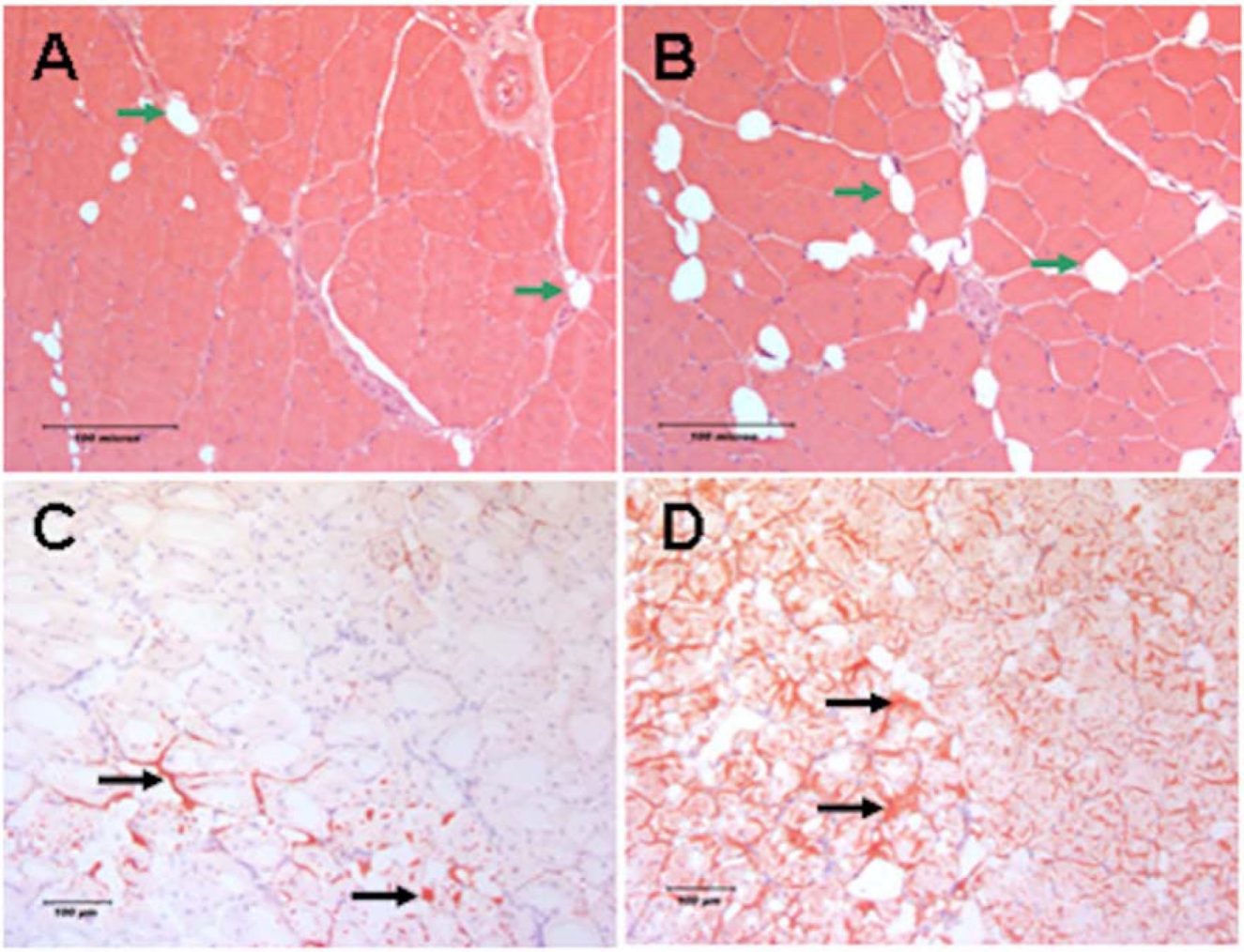

Figure 6. Histologic evaluation of skeletal muscle regeneration following IR

Representative images of regenerating TA muscle cross section obtained 28 days after IR. Images A and B are 200× H & E stained muscle from ND and DIO respectively. Regenerating myofibers present centrally localized nuclei. Green arrows indicate intramuscular adipocytes. There was significantly less centrally nucleated fibers and higher fat area measured in the DIO group compared to ND. Images C and D are 100× Oil Red O stained frozen TA muscle cross sections from ND and DIO mice respectively. Black arrows indicate fat accumulated between the myofibers. There is more extensive Oil Red O staining observed in the DIO muscle cross sections compared to ND indicating more fat accumulation in the tissue 28 days after IR.

NIH-PA Author Manuscript

NIH-PA Author Manuscript

NIH-PA Author Manuscript

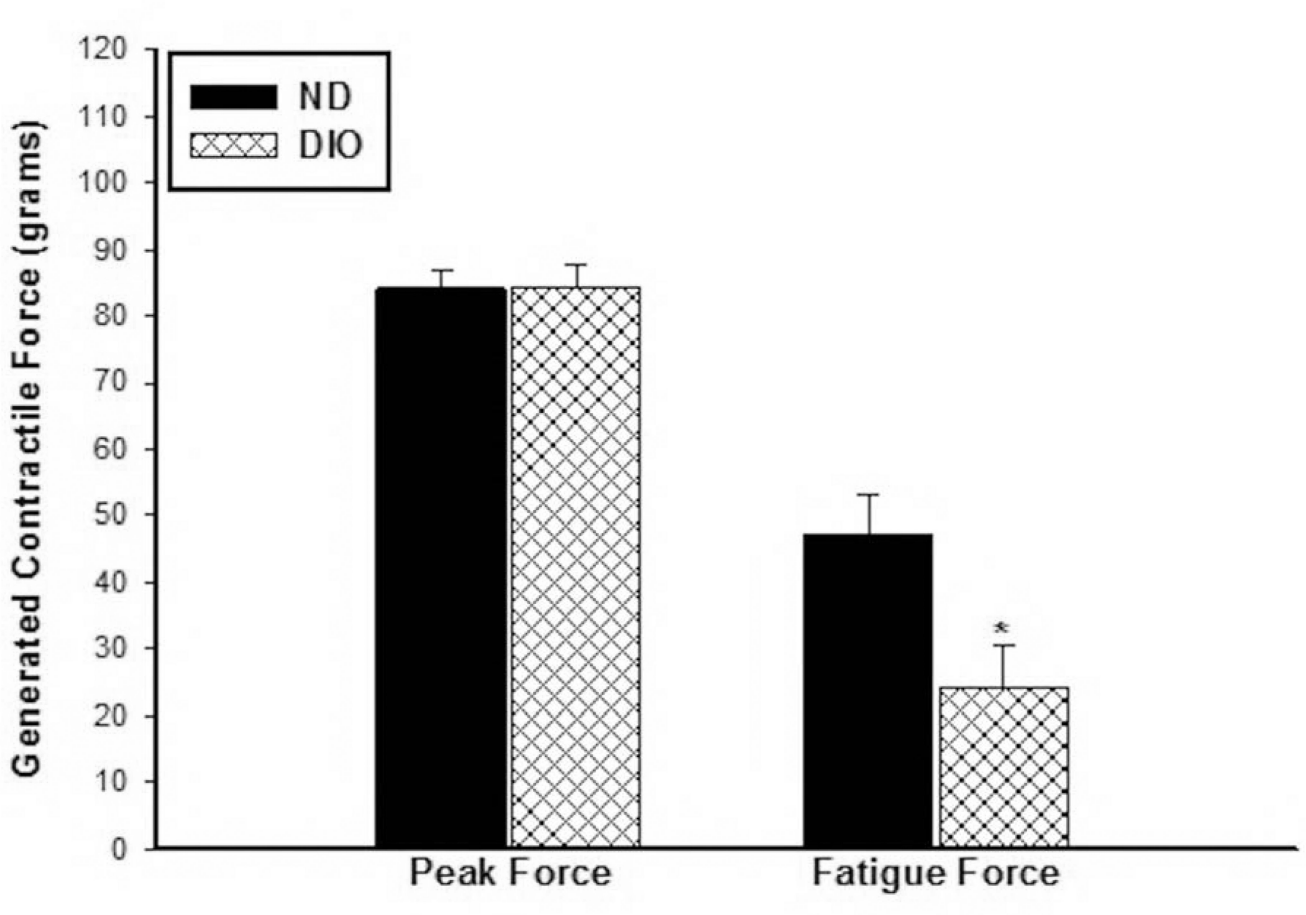

Figure 7. Assessment of hind limb function by direct muscle electrical stimulation

The acquired peak forces were similar in the two groups. However, the DIO mice generated significantly lower contractile forces at the end of the 10 minutes stimulation period compared to ND group indicating worsened fatigue contractile response (* p=0.022, n=6).

NIH-PA Author Manuscript

NIH-PA Author Manuscript

NIH-PA Author Manuscript

Table 1

Day 1 data summary for the hind limb perfusion, acute muscle fiber injury and markers of inflammation and thrombosis obtained 1 day following IR.

	DIO Day1 (n=6)	ND Day1 (n=7)	P value
Perfusion Ratio	1.47±0.09	1.27±0.12	P=0.43
% Injured Fibers	23.2±2.9	22.3±2.6	P=0.8
KC (pg/mg)	52.96±18.43	18.59±3.01	* p=0.008
MPO ng/mg	29.42±0.83	19.41±2.03	* p=0.0013
Neutrophils cell/hpf	56.78±4.51	24.41±3.73	* p=0.00017
TAT III (ng/mg)	0.195±0.009	0.117±0.012	* p=0.0005

NIH-PA Author Manuscript

NIH-PA Author Manuscript

NIH-PA Author Manuscript

Table 2

Data summary for hind limb perfusion ratio, markers of skeletal muscle fibers regeneration and cross sectional area (CSA) obtained at 28 days following IR.

	DIO Day28 (n=6)	ND Day28 (n=6)	P value
Perfusion Ratio	0.860±0.082	0.859±0.087	NS
Average Fat Area μm^2	8589.2±1314.6	2987.3±849.6	P=0.005
% Central Nuclei	72.8±2	81.6±0.9	P=0.0026
Fiber CSA μm^2	1347.8±258.7	1097.6±68	0.69